Using magnetic circular dichroism for the study of the magnetization and the magnetic moments of atoms in $Nd_3Fe_{27.5}Ti_{1.5}$

2009 J. Phys.: Condens. Matter 21 236001

(http://iopscience.iop.org/0953-8984/21/23/236001)

J. Phys.: Condens. Matter **21** (2009) 236001 (7pp) doi:10.1088/0953-8984/21/23/236001

Using magnetic circular dichroism for the study of the magnetization and the magnetic moments of atoms in $Nd_3Fe_{27.5}Ti_{1.5}$

C Sarafidis[1], F Wilhelm[2], A Rogalev[2], M Gjoka[3] and O Kalogirou[1]

[1] Department of Physics, Aristotle University of Thessaloniki, 54 124 Thessaloniki, Greece
[2] European Synchrotron Radiation Facility (ESRF), BP 220, 38043 Grenoble Cedex, France
[3] NCSR Demokritos, Institute for Materials Science, 153 10 Agia Paraskevi, Athens, Greece

Received 19 March 2009, in final form 6 April 2009
Published 7 May 2009
Online at stacks.iop.org/JPhysCM/21/236001

Abstract
An element-specific study of the $Nd_3Fe_{27.5}Ti_{1.5}$ compound using the hard x-ray magnetic circular dichroism (XMCD) technique is presented. The Nd L_2 and L_3 edge XMCD, as well as the Fe K edge XMCD, were measured in a magnetically oriented sample, parallel and perpendicular to its alignment direction. The XMCD spectra were recorded at three different temperatures, above, below and in between the characteristic peaks that the specific compound presents in AC susceptibility measurements. By probing the Nd L edges and the Fe K edge XMCD, we found that the dipolar R(5d)–Fe(3d) exchange interaction behaves differently with temperature change than the Fe–Fe magnetic interaction. Those differences appear to be in the vicinity of the AC susceptibility characteristic peaks. An XMCD signal was recorded at the Ti K edge, revealing a small orbital polarization due to the hybridization with Fe atomic states. This demonstrates the existence of a small finite magnetic moment in Ti atoms.

(Some figures in this article are in colour only in the electronic version)

1. Introduction

The $R_3(Fe, M)_{29}$-type family of compounds (3:29) present various interesting phenomena due to their complex monoclinic structure. They have been studied systematically because of their potential permanent magnet applications and their intrinsic magnetic properties [1–12]. The $Nd_3(Fe, Ti)_{29}$-type compounds crystallize in the $A2/m$ space group [1]. The monoclinic 3:29 structure has a high complexity; it contains 11 non-equivalent iron crystallographic sites and the fact that it can be considered as an intermediate phase between 1:12 and 2:17R structure types suggests bright prospects for the study of the field of exchange interactions in rare earth–transition metal intermetallic compounds. $Nd_3Fe_{27.5}Ti_{1.5}$ presents two transitions in the AC susceptibility curves, at 233 K and 160 K [1, 2]. The lower temperature transition is attributed to first-order magnetization phenomena (FOMP). However, there are contradictory explanations for the transition at 233 K. It has been reported to arise due to a spin reorientation transition (SRT) [2] although there is strong experimental evidence that a SRT does not exist at that temperature [1, 3, 4]. Using point-charge calculations, Li *et al* [5] have reported that in 3:29 systems there are two opposing rare earth sublattices which may result in a canted magnetic structure. In the 3:29 compounds the magnetocrystalline anisotropy is due to the competing contributions of the two sublattices, the rare earth and the transition metal sublattice. In $Nd_3Fe_{27.5}Ti_{1.5}$ the nature of the magnetocrystalline anisotropy was initially considered to have planar character with the easy magnetization direction (EMD) lying on the basal plane of the underlying 1:5 structure [2], while later studies have revealed the presence of a more complex tilted structure [1, 3, 4, 9]. In those references it has been shown that an easy cone type of anisotropy is present, the cone axis being the [4 0 $\bar{2}$] crystallographic direction of the monoclinic structure. The [4 0 $\bar{2}$] direction is related to the c-axis of the 1:12 phase and lies perpendicular to the [2 0 4] direction, which is related to the c-axis of the 2:17 phase, and to the [0 4 0] direction, which lies in the basal plane of the 2:17 phase [1]. Thus, the [2 0 4] and [0 4 0] directions are considered to be the hard directions of the compound.

The XMCD technique has been proven to be a very important tool in the research into magnetism. It is as an element-specific and shell-selective magnetic probe, since the XMCD intensity is quantitatively related to the local spin and orbital magnetic moments. In the rare earth–transition metal intermetallic compounds the rare earth conduction band electrons (5d) are very important, since they participate in the exchange interactions between the rare earth and transition metal sublattices. Their observation with the XMCD technique through experiments at the L_2 and L_3 edges of the rare earth atoms can provide valuable information on these interactions, although they cannot be explained with simple sum rules [13]. With the development of time dependent density functional theory (TDDFT) and its subsequent refinements, predictions of the electronic absorption (EA), electronic circular dichroism (ECE) and magnetic dichroism (MCD) spectra are now feasible, not only for the gas phase/isolated state, but also for solution, using the continuum solvent (environment) approach. The Dalton *ab initio* and DFT code has implemented the simulation of the EA, ECD and MCD spectra [14]. Up to now, as regards rare earth–iron intermetallic compounds, XMCD results are limited to the systematic study of the $R_2Fe_{14}B$ and the $RFe_{11}Ti$ series [15–19]. These results indicate that there is a rare earth contribution to the Fe K edge XMCD, and that this contribution reflects the magnetic state of the R atoms. Hence, it is necessary to extend previous research to different R–Fe intermetallic series to establish a better understanding of the characteristics of the XMCD signals in R–Fe intermetallic compounds. In the present work we present an investigation of the $Nd_3Fe_{27.5}Ti_{1.5}$ compound using the x-ray magnetic circular dichroism (XMCD) technique in order to extend the study of the magnetic interactions in this compound and to further clarify the nature of the magnetic transitions observed at low temperatures.

2. Experimental details

Alloys with $Nd_3Fe_{27.5}Ti_{1.5}$ nominal stoichiometry were prepared by arc-melting appropriate amounts of high purity metals, under an Ar atmosphere. The samples were melted twice in order to achieve better homogenization. Then the samples were wrapped in tantalum foil, encapsulated in evacuated quartz tubes, and annealed for 72 h at 1373–1473 K, and this was followed by water quenching. X-ray powder diffraction (XRD) with Cu Kα radiation and magnetization versus temperature measurements carried out at a field of 100 mT using a vibrating sample magnetometer were used for a first characterization of the samples. Most of the samples were found to be practically single phase with the monoclinic 3:29 structure and very small amounts of α-Fe. One sample was chosen for further analysis, with α-Fe content less than 1.5 wt% and crystallographic parameters $a = 10.645(2)$ Å, $b = 8.592(1)$ Å, $c = 9.752(2)$ Å, $\beta = 96.93(1)^\circ$ and $V = 885.41$ Å^3. The crystallographic parameters were calculated with Rietveld analysis and the Curie temperature of the material was found to be 420 K, from the thermomagnetic measurements. All these values are typical for the $Nd_3Fe_{27.5}Ti_{1.5}$ compound [1]. The bulk material was pulverized to fine powder with average particle size less than 37 μm and magnetically oriented samples were prepared under a magnetic field of 1 T. The powder was mixed with epoxy resin at RT and during the alignment process the sample was rotating with the rotational axis perpendicular to the external magnetic field; thus the rotational axis corresponded to the hard magnetization direction. The sample was carefully cut in order to allow it to be fixed on the sample holder of the XMCD apparatus. XMCD measurements were conducted using the beamline ID12 [20], which is dedicated to polarization dependent spectroscopies, at the European Synchrotron Radiation Facility (ESRF). The x-ray absorption near-edge structure (XANES) spectra at the Nd $L_{3,2}$ edges, Fe K edge and Ti K edge were measured in the total fluorescence yield mode, using a Si photodiode in a back-scattering geometry. A magnetic field of up to 3 T was applied parallel to the incident beam direction, using a superconducting cryomagnet. The XMCD spectra were obtained as a direct difference of two XANES spectra recorded successively with right and left circularly polarized x-rays (by reversing the helicity of the incoming beam). Moreover, to ensure that the measured XMCD spectra are free of any experimental artifact, the data were collected for both directions of the external applied magnetic field (parallel and antiparallel to the incoming x-ray beam). The XMCD spectra were recorded at the Nd L_2 and L_3 edges, at the Fe K edge and at the Ti K edge, parallel and perpendicular to the magnetic alignment direction. The spectra were recorded at three different temperatures, room temperature, liquid nitrogen temperature and in the interval between the two AC susceptibility transitions, i.e., at 180 K. The Ti K edge spectrum was recorded only at room temperature in order to study the possible existence of an induced magnetic moment in the Ti atom due to the polarization of the surrounding electronic density.

3. Results and discussion

This section is divided into four parts. The first part deals with the XMCD measurements at the Nd $L_{3,2}$ edges recorded along the easy magnetization axis (parallel to the magnetically aligned direction of $Nd_3Fe_{27.5}Ti_{1.5}$) and along the hard magnetization axis (perpendicular to the magnetically aligned direction of the $Nd_3Fe_{27.5}Ti_{1.5}$), whereas the second part deals with the XMCD measurements at the Fe K edge along both easy and hard magnetization axis (hereafter easy and hard axis). In the third part, the thermal dependence is presented for both Nd and Fe. Finally, the fourth part deals with the XMCD measurements at the Ti K edge.

3.1. Nd $L_{3,2}$ edges XMCD

In figure 1 the XANES and XMCD spectra recorded at the Nd L_2 and L_3 edges along the easy and hard magnetization axes measured at room temperature (RT), that is 295 K, and under 3 T magnetic field are presented. The most obvious feature is a main positive peak for both Nd L_3 and L_2 edges. The sign and the shape of the XMCD spectra are similar to those of the corresponding ones at Nd L edges

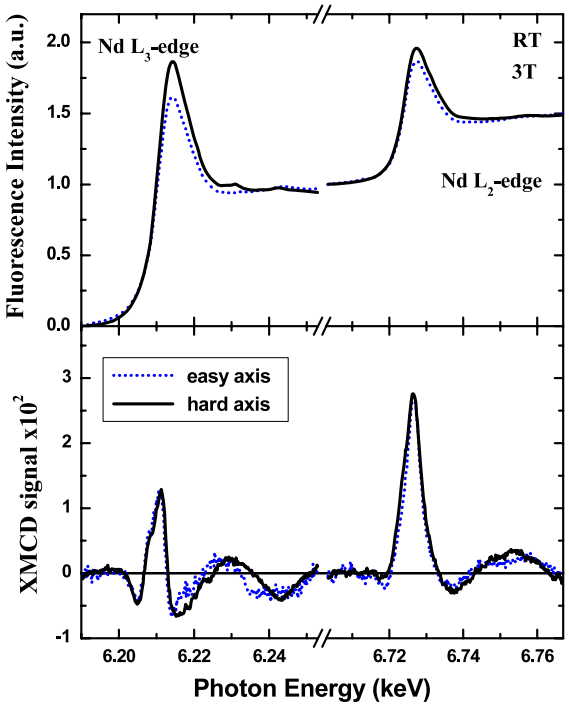

Figure 1. Normalized Nd $L_{3,2}$ edge XANES (upper panel) and XMCD (lower panel) spectra of $Nd_3Fe_{27.5}Ti_{1.5}$ compound recorded at room temperature (295 K) under 3 T magnetic field along the easy magnetization axis (dotted line) and along the hard magnetization axis (solid line).

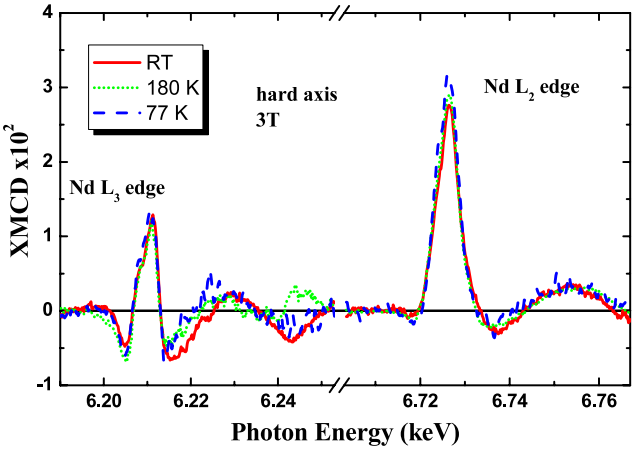

Figure 2. Temperature dependence of the Nd $L_{3,2}$ edge XMCD spectra of $Nd_3Fe_{27.5}Ti_{1.5}$ compound measured along the easy magnetization axis under 3 T magnetic field at 295 K (solid line), 180 K (dotted line) and 77 K (dashed line).

for other rare earth–transition metal intermetallic compounds like Nd–Fe–B [15–18]. The L_2 peak at around 6.725 keV is stronger, while the L_3 peak is centered around 6.21 keV. It has been previously shown by combining XMCD, x-ray resonant magnetic scattering and resonant inelastic x-ray scattering that those peaks correspond to dipolar transitions ($2p \rightarrow 5d$), whereas the features located at lower energies (6.205 and 6.209 keV for the L_3 edge, and 6.718 keV for the L_2 edge) correspond to quadrupolar transitions ($2p \rightarrow 4f$) [21]. We can first observe that the XANES spectra along the easy and hard magnetization axes are anisotropic since they do not have the same amplitude. This anisotropy in the XANES reflects the charge anisotropy mainly between the (a, b) plane and the $(c, a)/(c, b)$ plane of the unoccupied electronic density of states of the 5d shell of the Nd atoms. This effect arises for non-cubic crystallographic structure. The XMCD spectra are similar in shape and amplitude for easy and hard magnetization axes. Like those of Nd–Fe–B, the Nd and Fe magnetic moments are ferromagnetically coupled.

In figure 2 we show the XMCD spectra of the Nd $L_{3,2}$ edges measured along the easy magnetization axis at three different temperatures, 77 K, 180 K and RT. For these three temperatures we did not observe any sizable changes in the XANES spectra compared to the RT ones. In the following discussion we will focus essentially on the temperature dependence of the dipolar transition of the L_2 edge of Nd, which probes the 5d states. These states are strongly polarized due to the presence of a localized 4f magnetic moment at the Nd atoms via the Nd(4f)–Nd(5d) exchange interaction. Along the easy magnetization axis, we observe a sizable dependence of the main peak with temperature. The main peak intensity increases with decreasing temperature. The signal increases at 180 K by ∼39% compared to the one recorded at RT, whereas it increases by 49% at 77 K. Generally speaking, the XMCD intensity is proportional to the atomic magnetization projection along the incident x-ray beam direction. Since the XMCD technique is a vectorial magnetometry tool, changes in the XMCD intensity with temperature may reflect a corresponding change in the direction of the atomic magnetization and/or the temperature dependence of the magnetization. That increase with lowering temperature may appear, at first glance, to be due to the temperature dependence of the magnetization (the Curie temperature is 437 K); however at this stage one cannot safely exclude the possibility that the difference reveals the existence of a spin reorientation transition (SRT). It is of importance to notice that the shape and the sign of the whole spectra are not modified, showing that the Nd magnetic exchange coupling is the same in all temperatures.

If one looks at the XMCD signal of the L_2 edge corresponding to the quadrupolar transitions, the negative peak has practically a constant intensity. For the L_3 edge spectra the negative and positive peaks are weaker at room temperature, in accordance with the L_2 edge dipolar transition. In a detailed study of the well known $Nd_2Fe_{14}B$ rare earth transition metal compound, which certainly exhibits a spin reorientation transition, Chaboy *et al* have noticed that the negative peak corresponding to quadrupolar interaction weakens significantly above the SRT, both for the L_2 and the L_3 spectra [15]. They have indeed ascertained the multipolar nature of the different features in the XMCD spectra of Nd $L_{3,2}$ edges and verified that across the SRT, the dipolar and quadrupolar transitions possess different angular dependences as expected theoretically [22]. In our case, at the L_3 edge, the temperature dependence of the XMCD signal, both dipolar and quadrupolar parts, scales well, linearly, with the dipolar transition observed at the L_2 edge. Since the L_3 edge quadrupolar and dipolar transitions and the L_2 edge dipolar transitions exhibit the same

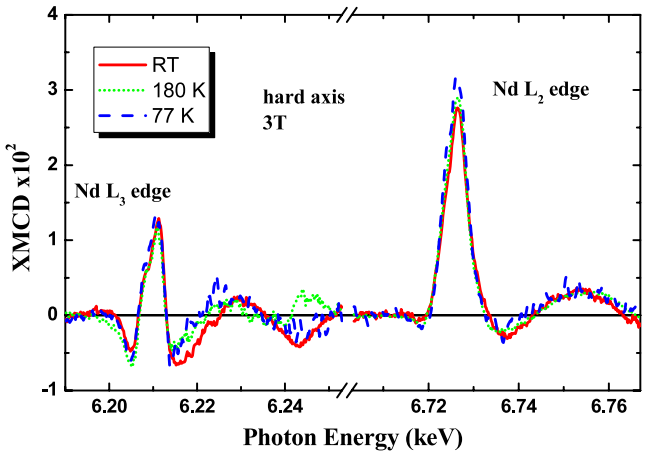

Figure 3. Temperature dependence of the Nd $L_{3,2}$ edge XMCD spectra of $Nd_3Fe_{27.5}Ti_{1.5}$ compound measured along the hard magnetization axis under 3 T magnetic field at 295 K (solid line), 180 K (dotted line) and 77 K (dashed line).

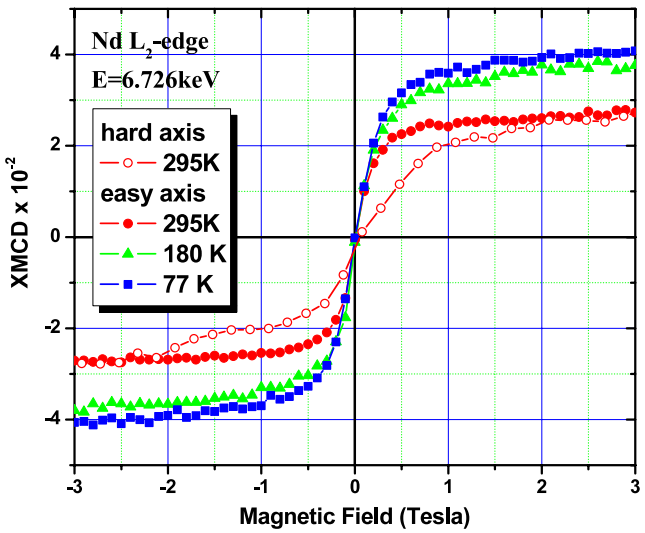

Figure 4. Magnetic field dependence of the XMCD signal at the Nd L_2 edge ($E = 6.726$ keV) recorded along the easy magnetization axis at 295 K (full circle), at 180 K (full triangle) and 77 K (full square). For comparison, also plotted is the magnetic field dependence of the XMCD signal at the Nd L_2 edge recorded along the hard magnetization axis at 295 K (open circle).

temperature dependence within the experimental accuracy, this means clearly that there is no SRT within the temperature range from RT to 77 K. They follow the temperature dependence of the macroscopic magnetization. The situation for the quadrupolar transitions at the L_2 edge is more ambiguous, since they do not change with temperature.

The XMCD spectra recorded at Nd $L_{3,2}$ edges measured along the hard magnetization axis at three different temperatures, 77 K, 180 K and RT, are presented in figure 3. The main characteristics of the XMCD spectra are the same as those corresponding to the easy magnetization axis. The most notable feature is the less pronounced increase of the L_2 main positive peak (dipolar transition) at low temperature compared to the easy axis case. At low temperature, the XMCD intensity for the hard and easy axes are 3.2×10^{-2} and 4.1×10^{-2}, respectively, compared to the edge jump. This difference may be due to the non-saturation of the magnetization under 3 T external magnetic field. We observe the same tendency within the measurement's accuracy at the L_3 edge of Nd. A small temperature variation in the XMCD spectra is observed at both L_3 and L_2 edges. Like for the easy axis, the quadrupolar and dipolar transitions follow the same temperature variation which confirms that there is no SRT. In figure 4 the field dependence of the maximum XMCD intensity at the Nd L_2 edge along the easy and hard axes is shown. The field dependence of the Nd magnetization follows the macroscopic magnetization curve. Along the easy axis, the curvatures of the Nd magnetization curves are the same for the three temperatures. No peculiarity is observed. Both Nd magnetization curves at RT correspond to the macroscopic ones measured using a SQUID [1].

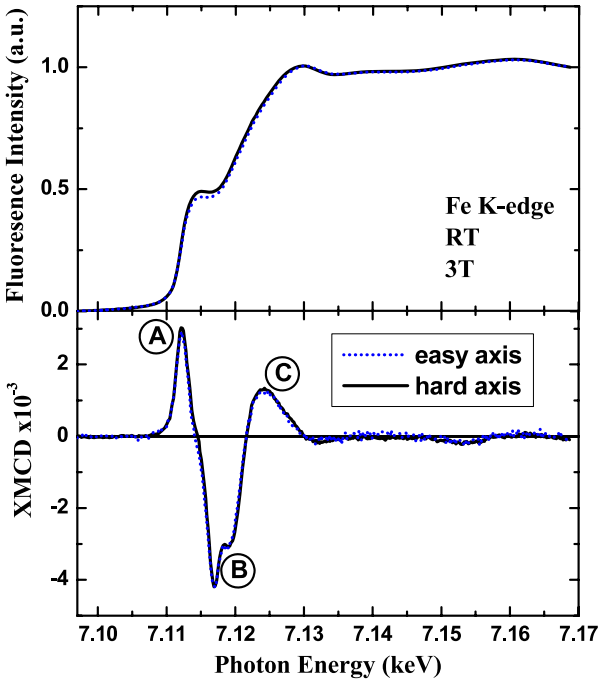

Figure 5. Normalized Fe K edge XANES (upper panel) and XMCD (lower panel) spectra of $Nd_3Fe_{27.5}Ti_{1.5}$ compound recorded at room temperature (295 K) under 3 T magnetic field along the easy magnetization axis (dotted line) and along the hard magnetization axis (solid line).

3.2. Fe K edge XMCD

In figure 5 the XANES and XMCD spectra recorded at the Fe K edge along the easy and hard axes measured at room temperature and under 3 T magnetic field are presented. The XANES and XMCD spectra are similar to the ones recorded for other rare earth–transition metal intermetallics [16]. The main feature is a negative peak at about 7.115 keV, surrounded by two smaller positive peaks. The narrow positive peak A at the absorption threshold ($E = 7.112$ keV) was assigned to the Fe sublattice magnetism, whereas the broad negative peak B and positive peak C above are due to the dipolar

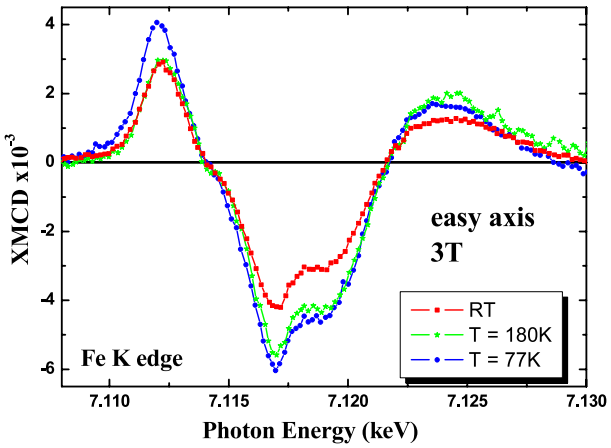

Figure 6. Temperature dependence of the Fe K edge XMCD spectra of $Nd_3Fe_{27.5}Ti_{1.5}$ compound measured along the easy magnetization axis under 3 T magnetic field at 295 K (solid line), 180 K (dotted line) and 77 K (dashed line).

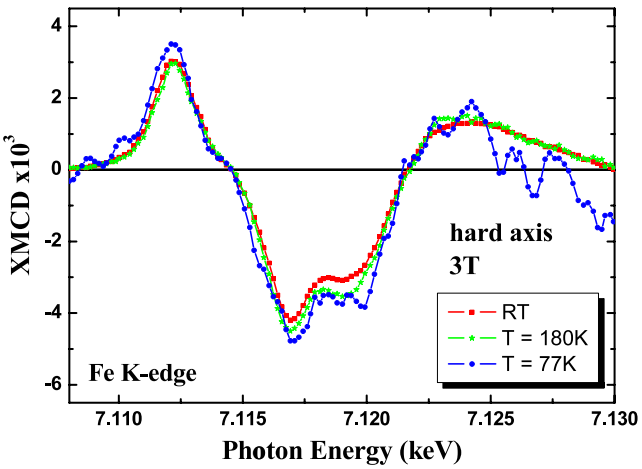

Figure 7. Temperature dependence of the Fe K edge XMCD spectra of $Nd_3Fe_{27.5}Ti_{1.5}$ compound measured along the hard magnetization axis under 3 T magnetic field at 295 K (solid line), 180 K (dotted line) and 77 K (dashed line).

interaction and reflect the exchange coupling between Nd and Fe atoms [23] and have been observed in the structurally related 2:14:1 [16] and 1:12 [19] rare earth–iron intermetallic compounds. Chaboy *et al* have shown that those peaks are due to the hybridization of the outermost states of the absorbing Fe with the 5d states of the rare earth neighbors and depend on the kind of the rare earth [19]. Our results extend the observation of this kind of interaction in the 3:29 rare earth–iron intermetallic compounds. We can observe that the XANES spectra for the probed easy and hard axes are similar, unlike those for the Nd L edges. Despite the non-cubic symmetry, no real electronic anisotropy is seen as for Nd atoms that are sitting on highly anisotropic sites. Further, the XMCD signal shape and amplitude are the same as those already observed for the XMCD at the Nd L edges.

In figure 6 the XMCD spectra of the Fe K edge measured along the easy magnetization axis at three different temperatures, 77 K, 180 K and RT, are shown. We can observe that the different features behave differently as a function of the temperature. The XMCD intensity of the peak A, that is considered to arise exclusively from the Fe atoms [19], increases very slightly from RT to 180 K and then strongly at 77 K, whereas the broad peak B increases strongly from RT to 180 K and then very slightly from 180 to 77 K. The temperature behavior of the feature C is rather like that of the broad peak B.

Figure 7 shows the XMCD spectra of the Fe K edge measured along the hard magnetization axis at three different temperatures, 77 K, 180 K and RT. Comparing with the easy magnetization axis case, the intensity difference with varying temperature of the different features is less pronounced. The XMCD intensities of peak A are very similar at RT and 180 K and increased at 77 K, whereas the broad peak B increases nearly linearly from RT to 77 K. The temperature behavior of the feature C is less easy to describe. In figure 8 the field dependence of the XMCD intensity recorded at the peak B (7.117 keV) at the Fe K edge, along the easy and hard axes, is presented. This field dependence of the Fe magnetization

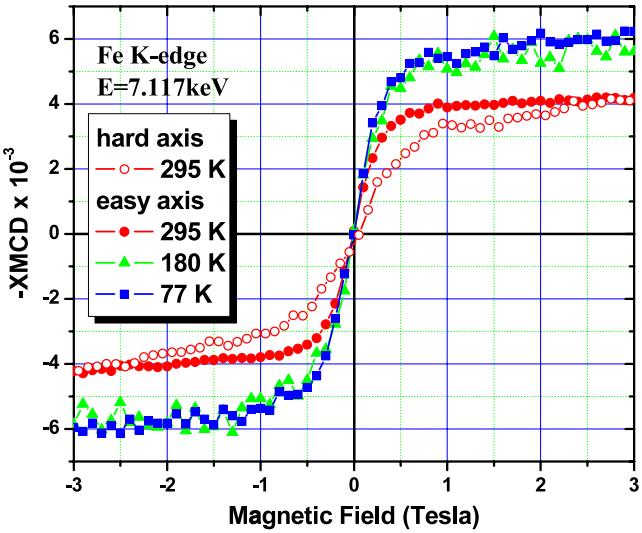

Figure 8. Magnetic field dependence of the XMCD signal at the Fe K edge ($E = 7.117$ keV) recorded along the easy magnetization axis at 295 K (full circle), at 180 K (full triangle) and 77 K (full square). For comparison, we have also plotted the magnetic field dependence of the XMCD signal at the Fe K edge recorded along the hard magnetization axis at 295 K (open circle).

follows the macroscopic magnetization curve. Along the easy axis, the curvatures of the Fe magnetization curves are the same for the three temperatures. No peculiarity is observed. Both Fe magnetization curves at RT correspond to the macroscopic ones measured using a SQUID [1].

3.3. Discussion

If one compares the element-specific magnetization curves measured at the Nd L_2 edge and Fe K edge for the three different temperatures, along the easy and hard axes, one can indeed observe that their respective field dependences (e.g. curvature and slope at high field) are exactly similar.

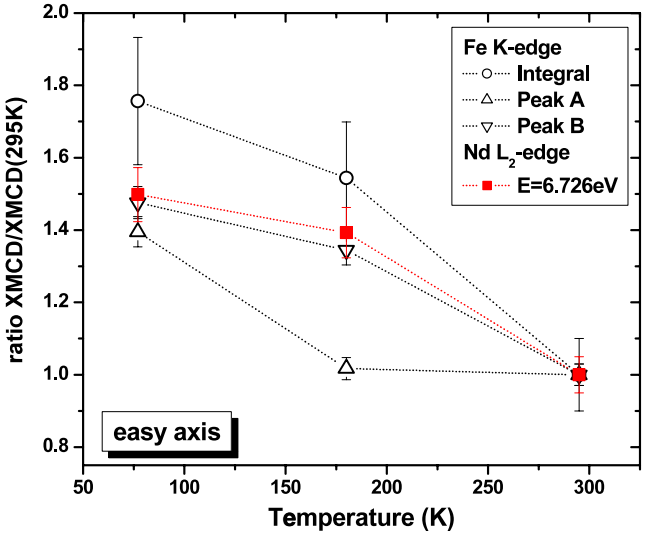

Figure 9. Temperature dependence of the normalized ratio to 295 K of the XMCD intensity recorded at the Fe K edge at peak A (triangle up), peak B (triangle down) and the Fe K edge XMCD integral (open circle) in comparison to the normalized ratio, to the 295 K value, of the XMCD signal at the Nd L_2 edge measured along the easy magnetization axis under 3 T.

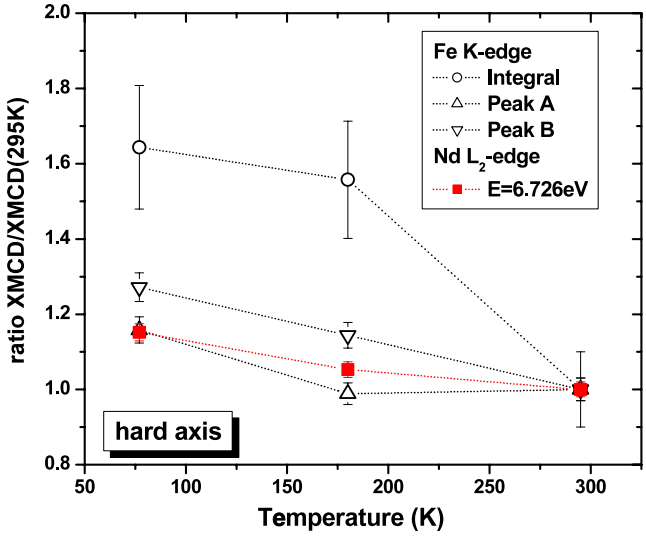

Figure 10. Temperature dependence of the normalized ratio, to the 295 K value. of the XMCD intensity recorded at the Fe K edge at peak A (triangle up), peak B (triangle down) and the Fe K edge XMCD integral (open circle) in comparison to the normalized ratio, to the 295 K value, of the XMCD signal at the Nd L_2 edge measured along the hard magnetization axis under 3 T.

This demonstrates that Fe and Nd magnetization sublattices are coupled and are collinear to each other. From the temperature dependence of the XMCD, one can observe changes in the spectral shape of the Fe K edge. We found that the temperature behavior of the broad XMCD peak B is similar to the temperature dependence of the Nd L_2 edge XMCD. Let us recall what one measures via the dichroism at the K edge. It was first pointed out by Gotsis and Strange [24] and Brooks and Johansson [25] that the K edge XMCD spectrum reflects the orbital polarization of the p states in the differential form $\mathrm{d}\langle L_z\rangle/\mathrm{d}E$ (where $\langle L_z\rangle$ is the ground state expectation value of the z component of the 4p orbital magnetic moment). In its integral form, the XMCD at the K edge is then a measure of the orbital magnetism of the 4p shell of Fe (considering only dipolar transitions). This leads to a rather simple and straightforward interpretation of the Fe XMCD spectrum at the K edge [26, 27]. The orbital polarization in the p symmetric states is in our case induced by the spin polarization in the p symmetric states through the spin–orbit interaction, and also by the orbital polarization at neighboring sites through hybridization [26]. In figure 9, we have plotted the normalized (to RT) XMCD intensity as a function of the temperature for peak A (7.112 eV), peak B (7.117 eV) and the XMCD integral at the Fe K edge in comparison to the maximum XMCD intensity at the Nd L_2 edge along the easy magnetization axis. We can observe that the intensity variation with temperature of the XMCD peak B at the Fe K edge XMCD and the maximum XMCD signal at the Nd L_2 edge are similar. Since the origin of peak B in the Fe K edge XMCD is mainly due to the orbital polarization of the neighboring Nd sites via the Fe(3d)–Nd(5d) hybridization, it is not surprising that it follows the same thermal dependence as the Nd sublattice magnetization. The temperature dependence of peak A in the XMCD at the Fe K edge does not follow the Nd sublattice magnetization. The origin of peak A in the Fe K edge XMCD, as mentioned above, is essentially the 3d orbital polarization at neighboring Fe sites that induces the orbital polarization through the p–d hybridization [26]. We then also represented the integral of the Fe K edge XMCD since it reflects the orbital magnetization. There we see that the 4p orbital polarization (and consequently the magnetization) of the Fe sublattice follows similarly the temperature dependence of the Nd sublattice magnetization. We can note that a change in the Nd–Fe exchange interaction appears between RT and 180 K, whereas a change in the Fe–Fe magnetic interaction appears below, between 180 and 77 K. Those modifications appear in the vicinity of the two characteristic temperature peaks in the AC susceptibility.

The same observations also apply for the spectra recorded along the hard magnetization axis (figure 10). If one compares the two temperature dependences along the easy and hard magnetization axes, one can see that Fe behaves similarly in the two directions whereas for Nd there are subtle changes that could be due to small changes in the magnetic anisotropy of Nd (related to the anisotropy of the orbital magnetic moment of Nd, that is the difference in orbital magnetic moment between the easy and hard magnetization axes) reflecting a possible change in the Nd sublattice magnetic structure.

3.4. Ti K edge XMCD

In figure 11 the Ti K edge XMCD and XANES spectra are presented. The spectra were recorded at 295 K along the hard magnetization axis direction. A weak negative peak at 4.97 keV with width of about 6 eV is observed and an amplitude of 4×10^{-3} compared to the edge jump of unity. Moreover, a small positive signal is observed at the

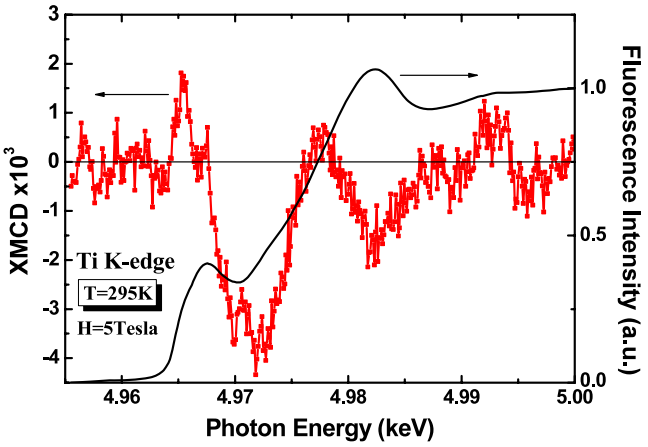

Figure 11. Normalized Ti K edge XANES (line, left scale) and XMCD (square, right panel) spectra of $Nd_3Fe_{27.5}Ti_{1.5}$ compound recorded at room temperature (295 K) under 5 T magnetic field along the hard magnetization axis.

pre-edge peak. The spectral shape and amplitude of the Ti K edge XMCD are very similar to those of the XMCD Fe K edge observed here. This existence of a non-zero XMCD integral reveals the existence of small finite 4p orbital polarization of the Ti atoms. Consequently, the Ti atoms present a net magnetic moment, possibly due the polarization of the electronic states due to the corresponding Fe states via hybridization. Despite the fact that we cannot quantify the induced magnetic moment in Ti, its role in the magnetic interactions present in such materials is certainly far from being negligible.

4. Conclusions

In the present work the XMCD study of $Nd_3Fe_{27.5}Ti_{1.5}$ is presented. It has been shown that no spin reorientation transition occurs in this intermetallic compound throughout the whole temperature range from 295 down to 77 K. This excludes the possibility that the SRT lies at the origin of the characteristic peak at high temperature (233 K) present in the AC susceptibility. From our results, we show that the Fe–Fe magnetic interaction changes subsequently between 180 and 77 K, whereas the Nd–Fe exchange interaction changes between 295 and 180 K. This appears to be in the vicinity of the two characteristic peaks at high (235 K) and low temperature (160 K) present in the AC susceptibility. As mentioned above, by applying the time dependent density functional theory (TDDFT) and its subsequent refinements, predictions of the electronic absorption (EA), electronic circular dichroism (ECE) and magnetic dichroism (MCD) spectra can be obtained. However, this is beyond the scope of this report and will be the subject of our future work.

References

[1] Kalogirou O, Psycharis V, Saettas L and Niarchos D 1995 *J. Magn. Magn. Mater.* **146** 335
[2] Morellon L, Pareti L, Algarabel P A, Albertini F and Ibarra M R 1994 *J. Phys.: Condens. Matter* **6** L379
[3] Sarafidis C, Kalogirou O, Bakas T and Gjoka M 2004 *J. Magn. Magn. Mater.* **272–277** e1913
[4] Kalogirou O, Psycharis V and Niarchos D 1996 *Solid State Commun.* **97** 471
[5] Li H S, Cadogan J M, Davis R L, Margarian A and Dunlop J B 1994 *Solid State Commun.* **90** 487
[6] Shah V R, Markandeyulu G, Rama Rao K V S, Huang M Q, Sirisha K and McHenry M E 1998 *J. Magn. Magn. Mater.* **190** 233
[7] Huo G, Qiao Z, Rao G, Liang J and Shen B 1999 *J. Alloys Compounds* **285** 216
[8] Yang D, Wang J, Tang N, Shen Y and Yang F 1999 *Appl. Phys. Lett.* **74** 4020
[9] Kalogirou O, Sarafidis C, Gjoka M, Bakas T and Giannouri M 2001 *J. Alloys Compounds* **325** 59
[10] Wang J L, Marquina C, Ibarra M R, Wang W Q, Yang F M, Wu G H, Tegus O, Klaasse J C P, Brück E and de Boer F R 2003 *J. Appl. Phys.* **93** 6924
[11] Huo G Y, Rao G H, Qiao Z Y, Liu Q L, Chen X L, Liang J K and Shen B G 2000 *J. Phys.: Condens. Matter* **12** 1161
[12] Kalogirou O, Sarafidis C, Gjoka M and Litsardakis G 2002 *J. Magn. Magn. Mater.* **247** 34
[13] Schütz G, Knülle M, Wienke R, Wilhelm W, Wagner W, Kienle P and Frahm R 1988 *Z. Phys.* B **73** 67
[14] Solheim H, Frediani L, Ruud K and Coriani S 2008 *Theor. Chem. Acc.* **119** 231
[15] Chaboy J, Bartolomé F, Garcia L M and Cibin G 1998 *Phys. Rev.* B **57** R5598
[16] Chaboy J, Maruyama H, Garcia L M, Bartolomé F, Kobayashi K, Kawamura N, Marcelli A and Bozukov L 1996 *Phys. Rev.* B **54** R15637
[17] Chaboy J, Garcia L M, Bartolomé F, Marcelli A, Cibin G, Maruyama H, Pizzini S, Rogalev A, Goedkoop J B and Goulon J 1998 *Phys. Rev.* B **57** 8424
[18] Chaboy J, Garcia L M, Bartolomé F, Maruyama H, Marcelli A and Bozukov L 1998 *Phys. Rev.* B **57** 13386
[19] Chaboy J, Laguna-Marco M A, Sanchez M C, Maruyama H, Kawamura N and Suzuki M 2004 *Phys. Rev.* B **69** 134421
[20] Rogalev A, Goulon J, Goulon-Ginet C and Malgrange C 2001 *Magnetism and Synchrotron Radiation* (*Lecture Notes in Physics* vol 565) ed E Beaurepaire, F Scheurer, G Krill and J P Kappler (Berlin: Springer)
[21] Bartolomé F, Tonnerre J M, Sève L, Raoux D, Lorenzo J E, Chaboy J, Garca L M, Bartolomé J, Krisch M, Rogalev A, Serimaa R, Kao C C, Cibin G and Marcelli A 1998 *J. Appl. Phys.* **83** 7091
[22] Carra P and Altarelli M 1990 *Phys. Rev. Lett.* **64** 1286
Carra P *et al* 1991 *Phys. Rev. Lett.* **66** 2495
[23] Chaboy J, Piquer C, Plugaru N, Bartolomé F, Laguna-Marco M A and Plazaola F 2007 *Phys. Rev.* B **76** 134408
[24] Gotsis H J and Strange P 1994 *J. Phys.: Condens. Matter* **6** 1409
[25] Brooks M S S and Johansson B 1996 *Spin–Orbit Influenced Spectroscopies of Magnetic Solids* (*Lecture Notes in Physics* vol 466) ed H Ebert and G Schütz (Berlin: Springer) p 211
[26] Igarashi J I and Hirai K 1994 *Phys. Rev.* B **50** 17820
[27] Ebert H 1996 *Rep. Prog. Phys.* **59** 1665